Crossed molecular beam studies on the reaction dynamics of O (D 1) + N 2 O

Yu-Ju Lu, Chi-Wei Liang, and Jim J. Lin

Citation: The Journal of Chemical Physics **125**, 133121 (2006); doi: 10.1063/1.2202828
View online: http://dx.doi.org/10.1063/1.2202828
View Table of Contents: http://scitation.aip.org/content/aip/journal/jcp/125/13?ver=pdfcov
Published by the AIP Publishing

Crossed molecular beam studies on the reaction dynamics of $O(^1D)+N_2O$

Yu-Ju Lu and Chi-Wei Liang
Institute of Atomic and Molecular Sciences, Academia Sinica, Taipei 106, Taiwan
and Department of Chemistry, National Taiwan University, Taipei 106, Taiwan

Jim J. Lin[a)]
Institute of Atomic and Molecular Sciences, Academia Sinica, Taipei 106, Taiwan
and Department of Applied Chemistry, National Chiao Tung University, Hsinchu 300, Taiwan

(Received 21 March 2006; accepted 14 April 2006; published online 5 October 2006)

The reaction of oxygen atom in its first singlet excited state with nitrous oxide was investigated under the crossed molecular beam condition. This reaction has two major product channels, NO +NO and N_2+O_2. The product translational energy distributions and angular distributions of both channels were determined. Using oxygen-18 isotope labeled $O(^1D)$ reactant, the newly formed NO can be distinguished from the remaining NO that was contained in the reactant N_2O. Both channels have asymmetric and forward-biased angular distributions, suggesting that there is no long-lived collision complex with lifetime longer than its rotational period. The translational energy release of the N_2+O_2 channel (f_T=0.57) is much higher than that of the NO+NO channel (f_T=0.31). The product energy partitioning into translational, rotational, and vibrational degrees of freedom is discussed to learn more about the reaction mechanism. The branching ratio between the two product channels was estimated. The $^{46}N_2O$ product of the isotope exchange channel, $^{18}O+^{44}N_2O \rightarrow ^{16}O+^{46}N_2O$, was below the detection limit and therefore, the upper limit of its yield was estimated to be 0.8%. © *2006 American Institute of Physics*. [DOI: 10.1063/1.2202828]

I. INTRODUCTION

There is considerable experimental[1–13] and theoretical[14–25] attention on the reaction dynamics of $O(^1D)+N_2O$. The reaction has two major product channels which are highly exothermic:

$$O(^1D) + N_2O \rightarrow NO + NO, \quad \Delta H^0_{0\ K} = -81.9 \text{ kcal/mol}, \tag{R1}$$

$$\rightarrow N_2 + O_2(^1\Delta), \quad \Delta H^0_{0\ K} = -102.3 \text{ kcal/mol}. \tag{R2}$$

Both channels are fast (close to the gas kinetic limit) and without potential energy barriers. (R1) is thought to be the primary source of NO in the upper stratosphere, where highly reactive $O(^1D)$ is produced by UV photolysis of ozone. Because it is relatively more feasible to detect NO by spectroscopic methods such as laser induced fluorescence (LIF), resonance enhanced multiphoton ionization (REMPI), and Fourier-transform infrared (FT-IR) emission spectroscopy, most experimental studies have focused on (R1). To our knowledge, there is no experimental literature on the reaction dynamics of (R2) so far.

(R1) produces two NO molecules. Conventionally we call the newly formed NO that contains the incoming $O(^1D)$ atom the *new* NO and call the remaining NO the *old* NO. The exothermicity of (R1) corresponds to 17 quanta of NO vibrational energy. Early studies by the Simons group[3–5] investigated (R1) by LIF technique, especially Doppler-resolved, polarized LIF probing of NO products from velocity aligned $O(^1D)$ reactant[4,5] in cell conditions. The internal state-resolved translational energy distribution was analyzed from the Doppler profiles. They concluded that besides a complex mechanism producing intermediate NO vibrational levels (v=1–15), a substantial fraction of (R1) undergoes a stripping mechanism. In the stripping mechanism, the old NO is left rotationally and translationally cold (as a spectator) while the newly formed NO is vibrationally very hot and forward scattered. In particular, the new NO(v=16,17) +old NO(v=0) channel demonstrates the stripping mechanism.[5]

Kajimoto and co-workers have studied (R1) by LIF spectroscopy.[6–10] They measured the vibrational distributions of the new and old NO by using isotope labeled $^{18}O(^1D)$ reactant.[7] The new NO has a bimodal vibrational distribution and is vibrationally hotter than the old NO. The old NO still has a considerable population in high vibrational levels. They suggested a short-lived complex mechanism in which the energy redistribution between the new and old NO molecules is quite efficient.[7] The same group also found that the vibrational population of NO in v=11–17 decreases monotonically over this range,[8] which would not be expected if the stripping mechanism is significant. A recent work measured the rotational state distribution of NO (v=0,1,2) products. The rotational temperature was found to be very high and close to the prediction of phase space theory.[9] FT-IR (Ref. 11) and, recently, time-resolved FT-IR (Ref. 12) techniques have also been used to measure the NO vibrational population of (R1), resulting in similar NO vibrational distributions. Figure 1 shows a summary of the presently available NO

[a)]Author to whom correspondence should be addressed. Electronic mail: jimlin@gate.sinica.edu.tw

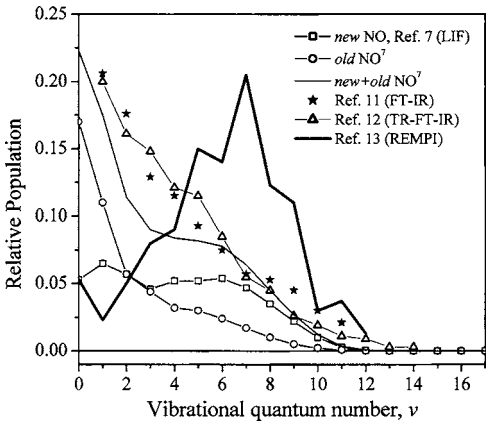

FIG. 1. Summary of available NO vibrational populations of (R1) measured by various groups.

vibrational populations measured by a few groups. While most cell experiments show that the total NO vibrational distribution is peaked near $v=0$, the Houston group[13] reported that the distribution is peaked at $v=7$. They used a single molecular beam technique to probe the rotationally cooled but vibrationally unquenched NO product of (R1) by $1+1'$ REMPI. The average vibrational energy is between 24 000 and 28 000 cm^{-1}, which is much greater than other literature values.[13]

There are several *ab initio* calculations on the potential energy surface (PES) of (R1) and (R2). Last *et al.*[14] used Moller-Plesset method to calculate the minimum energy paths of (R1) and (R2). The lowest $^1A'$ surface is attractive for both (R1) and (R2), while electronic excited surfaces might be unimportant at low collision energies. González *et al.*[15] used high level CASPT2 method to calculate the minimum energy paths near the entrance regions of (R1) and (R2). Reaction intermediates and transition states have been located by CASSCF method and single point energies were refined by CASPT2 method. A few intermediates were found for (R1), such as *trans*-ONNO, *cis*-ONNO, etc. Although some local minima have been located for (R2) by CASSCF method, they are likely only artifacts and do not exist at the CASPT2 level of theory.[15,16] Recently, Takayanagi and Akagi[17] have constructed a global potential energy surface at CASPT2/cc-PVDZ level of theory. On this surface, there is a deep well at the entrance region of (R1), but there is no significant well for (R2). From the CASPT2 global PES (Ref. 17) and minimum energy paths,[15] it can be seen that the preferred orientations of the attaching $O(^1D)$ atom are quite different for (R1) and (R2).

Some theoretical investigations have focused on NO dimers or N_2O_2 isomers. Low-lying electronic states of NO dimers have been investigated using MRCI and CASPT2 methods.[18] Structures and energies of various N_2O_2 isomers have been calculated by *ab initio* and density functional methods.[19]

Quasiclassical trajectory (QCT), transition state theory (TST), and quantum-classical calculations have been carried out on empirical surfaces as well as on *ab initio* potential energy surfaces.[15–17,20–24] A quantum-classical wave packet calculation[20] has been performed on the global CASPT2 PES.[17] The product branching ratio between (R1) and (R2) shows a significant dependence on the initial orientation angle, similar to a previous classical trajectory result[17] using the same surface. This initial orientation effect may explain why the product rovibrational distribution of (R1) from a laser-initiated half reaction experiment[6] is quite different from the full-collision case. The translational energy dependence has also been studied.[17,20] Furthermore, product rotational distributions of low vibrational NO ($v=0,1,2$) levels have been calculated by QCT methods[9] on this surface. While a "half-collision" QCT calculation, in which statistical distribution at the reaction intermediate is assumed, well reproduces the experimental rotational distributions, a "full-collision" QCT calculation made a poor prediction with too much rotational excitation. It may be due to poorly reproduced couplings between the stretching and bending/torsional motions on the PES.[9] A reduced dimensionality calculation,[21] in which the three stretching motions were fully treated at fixed initial and final orientation angles, shows that the new NO product is vibrationally hotter than the old NO.

N_2O is isoelectronic with CO_2. Recent crossed molecular beam studies[26,27] show that CO_2 exchanges isotopes with $O(^1D)$ atom very efficiently through two distinct mechanisms: a conventional electronic quenching isotope exchange, e.g., $Q(^1D)+CO_2 \rightarrow COQ+O(^3P)$, and a newly found nonquenching isotope exchange, e.g., $Q(^1D)+CO_2 \rightarrow COQ+O(^1D)$. Here Q denotes the ^{18}O isotope. *Ab initio* PES and RRKM calculations well support these two mechanisms.[28] It is, therefore, reasonable to imagine that N_2O could undergo an analogous isotope exchange with $O(^1D)$ atom,

$$Q(^1D) + N_2O \rightarrow N_2Q + O(^3P/^1D). \quad \text{(R3)}$$

The yield of (R3) may affect isotope modeling of stratospheric N_2O. There are debates about the significance of (R3) in the atmospheric isotope modeling.[29–32]

There are other energetically allowed product channels, such as $N+NO_2$, $N_2+2O(^3P)$, and $O(^3P)+N_2O$, which have very minor yields.[33] Recently, the yield of electronic quenching of $O(^1D)$ by N_2O has been determined to be 0.04 ± 0.02.[34]

In this report, we investigated the reaction dynamics of (R1) and (R2) by the crossed molecular beam method. Product translational energy distributions and angular distributions of (R1) and (R2) were measured. Possible reaction mechanisms are discussed by comparing the product energy partitioning into vibrational, rotational, and translational degrees of freedom. We also searched for the product of (R3).

II. EXPERIMENT

Most features of the crossed molecular beam apparatus have been described previously.[27] Only the relevant part of the experimental setup is mentioned here. An $O(^1D)$ atomic beam was generated by laser photolysis of a skimmed O_2 molecular beam at 157.6 nm, $O_2+h\nu(157.6\ nm)\rightarrow O(^1D)+O(^3P)$. The 30–50 mJ output of a F_2 excimer laser (Lambda Physik, LPX 210i, F_2 version) was focused by a

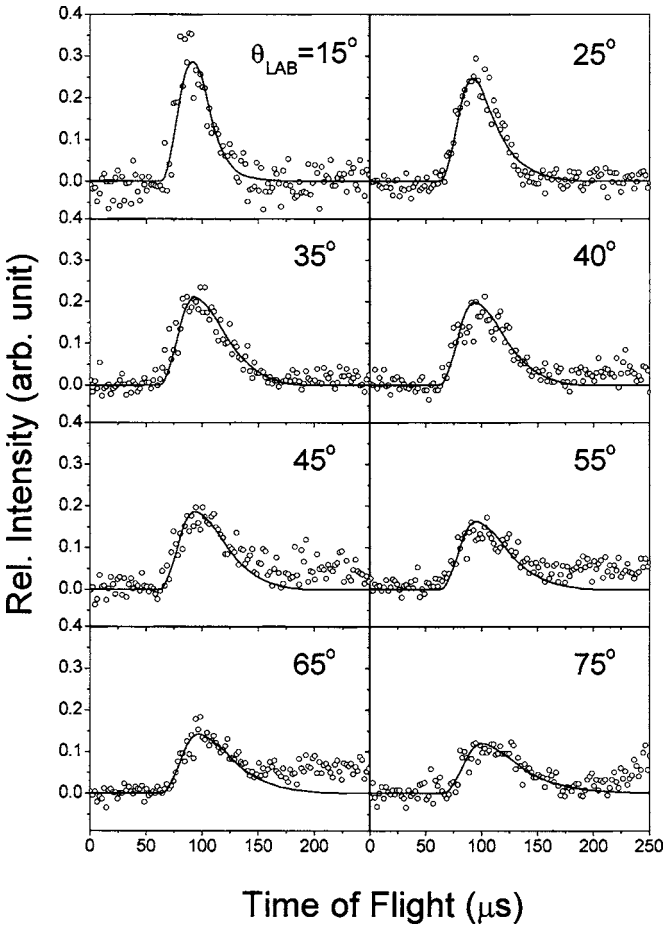

FIG. 2. Experimental TOF spectra of mass 32 probing the product from $^{18}O(^1D)+N_2O \rightarrow {}^{32}NO+{}^{30}NO$ reaction at several laboratory angles. Open circles: data, solid line: fit.

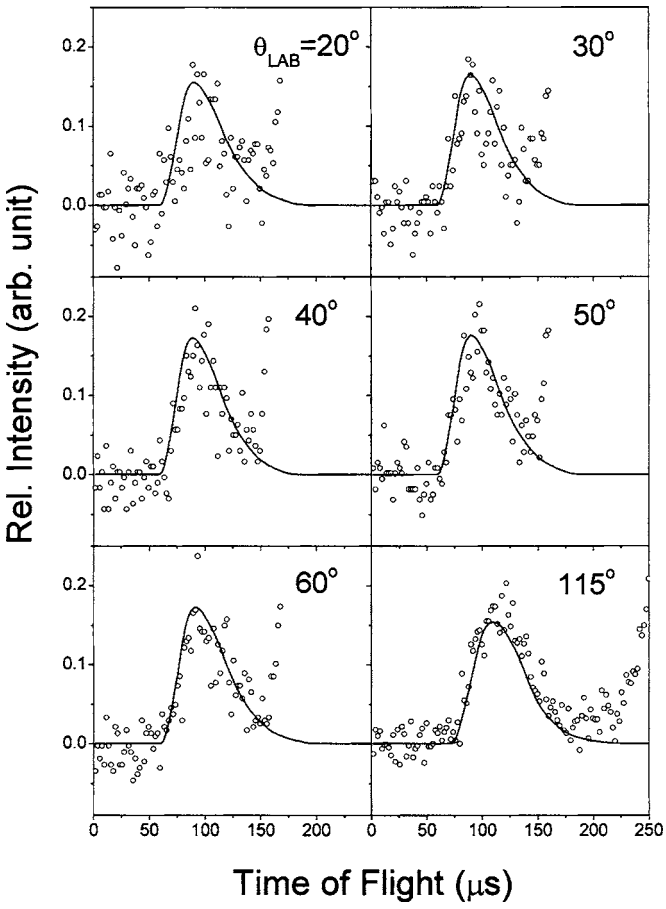

FIG. 3. Experimental TOF spectra of mass 30 probing the product from $^{18}O(^1D)+N_2O \rightarrow {}^{32}NO+{}^{30}NO$ reaction at several laboratory angles. Open circles: data, solid line: fit.

special cylindrical-spherical MgF_2 lens to a spot size of 3 $\times 3$ mm^2. Isotope labeled O_2 (^{18}O 97%) was used when an $^{18}O(^1D)$ atomic beam was needed. The $O(^1D)$ atomic beam had a very narrow velocity distribution ($<2\%$) and an angular divergence of about ±4° [full width at half maximum (FWHM)]. Besides $O(^1D)$ atoms, this atomic beam has an equal amount of $O(^3P)$ atoms. The reactivity of $O(^3P)$ atom toward N_2O is much lower than that of $O(^1D)$ atom.[35] Therefore it is safe to ignore contributions from the $O(^3P)$ atoms in the atomic beam.

A N_2O molecular beam was generated by expanding neat N_2O gas through a fast pulsed valve (Even-Lavie valve).[36] A sharp edge skimmer (Beam Dynamics Inc., 2 mm diameter) was used to define the angular divergence to about ±1.5° (FWHM). This pulsed valve produced a narrow pulse width of ~30 μs (FWHM, for N_2O gas pulse at the interaction region), which significantly reduced the effusive background gases from the beam source.

Two reactant beams crossed each other at a 90° angle. In the case of $^{18}O(^1D)$(2160 m/s)+N_2O(660 m/s) experiment, the collision energy was 7.8 kcal/mol. Scattered products traveled 24 cm and were then detected by a time-resolved quadrupole mass spectrometer. The electron impact ionizer of the mass spectrometer is located in a triple differentially pumped ultrahigh vacuum chamber (10^{-12} torr) to reduce background from residual gases and from the scattering chamber. Time-of-flight (TOF) spectra of the nascent products were recorded by a multichannel scalar (EG&G, Turbo MCS) with 2 μs time bins. Product velocity distributions were derived from the TOF spectra. Angular distribution was measured by rotating the whole detector. Trial product translational energy distribution $P(E_T)$ and angular distribution $P(\theta)$ in the center-of-mass (CM) frame were input to a forward convolution computer program to simulate the TOF spectra in the laboratory frame. The $P(E_T)$ and $P(\theta)$ were adjusted iteratively until a satisfactory fit to the experimental TOF spectra and angular distribution was obtained. Instrumental functions used in the program were properly determined by a series of calibration experiments, such as O_2 photolysis at 157.6 nm, O+Ne/Ar elastic scattering, etc.

III. RESULTS AND DISCUSSION

A. NO+NO channel and N_2+O_2 channel

Figure 2 shows experimental TOF spectra of the mass 32 product from a crossed molecular beam reaction of $^{18}O(^1D)+N_2O \rightarrow {}^{32}NO+{}^{30}NO$. Using an isotope labeled $^{18}O(^1D)$ beam, we can distinguish the newly formed ^{32}NO from the old ^{30}NO. The open circles represent the experimental data and the solid lines represent the fit simulated by the forward convolution program. Here the 0° laboratory

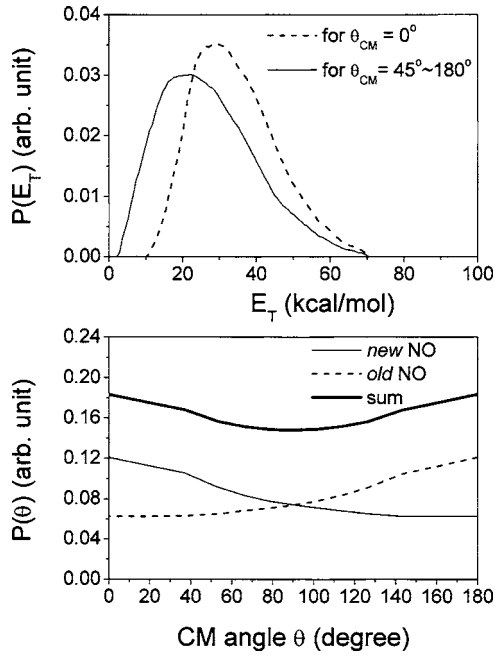

FIG. 4. Product translational energy distribution $P(E_T)$ and angular distribution $P(\theta)$ used to fit Figs. 2 and 3 for the reaction of $^{18}O(^1D)+N_2O \rightarrow {}^{32}NO+{}^{30}NO$ (R1).

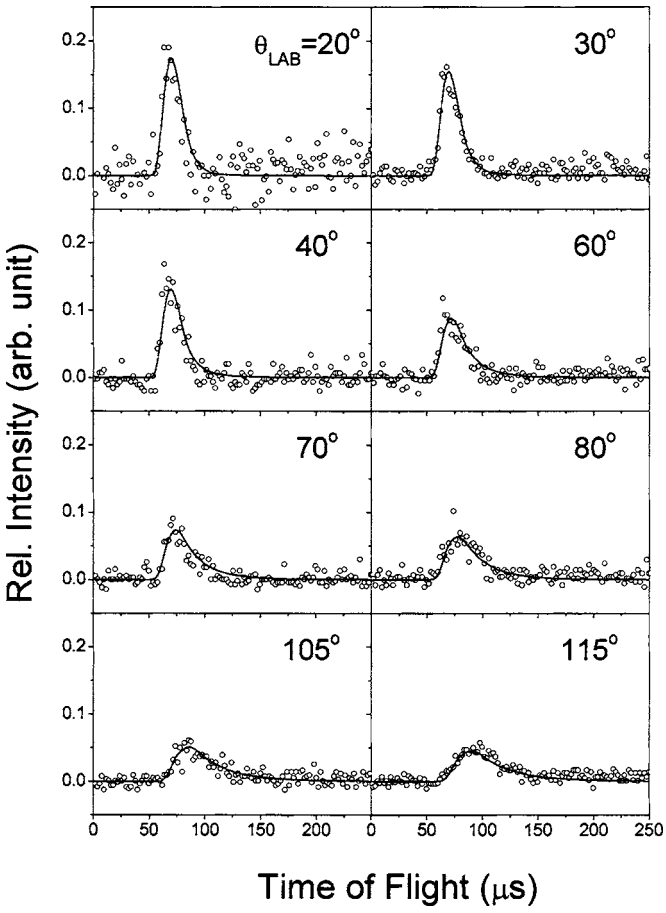

FIG. 5. Experimental TOF spectra of mass 34 probing the product from $^{18}O(^1D)+N_2O \rightarrow N_2+{}^{34}O_2$ reaction at several laboratory angles. Open circles: data, solid line: fit.

angle is defined as the direction of $O(^1D)$ velocity vector. The N_2O velocity is at 90° laboratory angle. The laboratory angle of the center of mass is about 37°. In Fig. 2, the TOF peaks corresponding to formation of the new NO show higher intensity at smaller laboratory angles. Some minor background that may come from N_2O molecular beam shows up at larger laboratory angles, but it is much slower than the signal peak. Figure 3 shows TOF spectra of mass 30, which represent the old NO product. Dissociative ionization of scattered N_2O in the electron impact ionizer produces large background at TOF longer than ~150 μs. Fortunately this background peak is slower and does not overlap with the signal peak. We have checked TOF spectra at mass 44 (N_2O^+) to confirm the source of background. This background also makes the TOF spectra noisier. Despite the background, we can clearly see that the old NO peaks have higher intensity at larger laboratory angles.

In the center-of-mass (CM) frame, the new NO and old NO have to be momentum matched, which means that they must fly in opposite directions. For example, a new NO flying in the forward direction ($\theta_{CM}=0°$) is matched with an old NO flying in the backward direction ($\theta_{CM}=180°$). Here, the forward direction is defined as the direction of the $O(^1D)$ velocity vector in the CM frame. With the TOF spectra of both new and old NO at wide-ranging laboratory angles, we can fit the product translational energy distribution $P(E_T)$ and angular distribution $P(\theta)$ in the CM frame. The result is plotted in Fig. 4. First, we tried to fit the data with a single $P(E_T)$, but we found that the new NO is slightly faster in the forward direction than at other θ_{CM}. Therefore we used a faster $P(E_T)$ in the forward direction for the new NO (dashed line in Fig. 4 upper) and a slower $P(E_T)$ for $\theta_{CM}=45°-180°$. For θ_{CM} between 0° and 45°, an interpolated $P(E_T)$ between the two $P(E_T)$'s was used. The angular distribution is shown in Fig. 4. By momentum matching, the $P(\theta)$ of the new NO and that of the old NO must be mirror images. The summation of the two $P(\theta)$'s was used to fit mass 30 data from an unlabeled experiment, $^{16}O(^1D)+N_2O \rightarrow {}^{30}NO+{}^{30}NO$. As expected, the fitting (not shown) is as nice as those in Figs. 2 and 3. In Fig. 4, we can see that the $P(\theta)$ for the new NO is quite broad and forward biased.

For (R2), the O_2 product was observed at mass 34 from the reaction of $^{18}O(^1D)+N_2O \rightarrow {}^{34}O_2+N_2$. The data and fit are shown in Fig. 5. The N_2 product could not be measured due to high background at mass 28 from residual CO gas in the detector chamber. Here we used ^{18}O labeled reactant to avoid background from residual O_2 gas in the scattering chamber. Compared with mass 32 (the new NO product), the mass 34 signal ($^{18}O^{16}O$) has a similar angular distribution, that is, higher intensity at smaller laboratory angles. Regarding the TOF peaks, the mass 34 is faster and sharper than the mass 32. The $P(E_T)$ and $P(\theta)$ of (R2) are shown in Fig. 6. Analogous to (R1), a faster $P(E_T)$ was used at the forward direction, and the $P(\theta)$ is broad and forward biased. The $P(E_T)$'s of (R2) are peaked at ~60 kcal/mol, much higher than those of (R1) (20–30 kcal/mol). Although (R2) has a higher exothermicity of 102 kcal/mol with respect to (R1) (exothermicity of 82 kcal/mol), the translational energy release of (R2) is still much more significant. It should reveal features of the potential energy surface, which are different

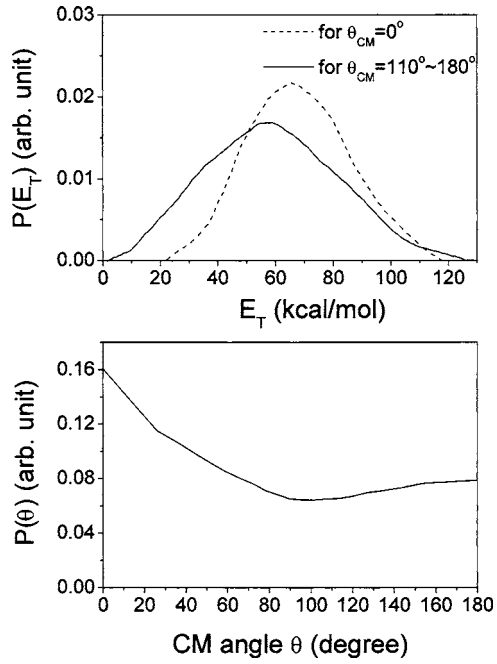

FIG. 6. Product translational energy distribution $P(E_T)$ and angular distribution $P(\theta)$ used to fit Fig. 5 for the reaction of $^{18}O(^1D)+N_2O \rightarrow N_2+^{34}O_2$ (R2).

for (R1) and (R2). For these two highly exothermic reactions, the majority of available energy is from the reaction exothermicity which corresponds to the drop of potential energy from reactant side to product side. Along the reaction coordinate of (R1), there is a very significant potential energy drop at the entrance valley. That is, the entrance well or intermediate of (R1) is quite stable relative to the reactants. There is no significant well in the entrance region of (R2). Along the reaction coordinate of (R2), there is a large and pronounced (clifflike) potential energy drop at the exit valley. These features can be seen on the three-dimensional minimum energy paths calculated by Last *et al.*[14] and on the global PES at CASPT2/cc-PVDZ level of theory.[17] This level of CASPT2 calculation has been confirmed by other CASPT2 calculations using a larger active space and/or other basis sets.[15,16] On this PES, there is a deep entrance well for (R1). When NNO is fixed at the equilibrium geometry of a N_2O molecule, the entrance well is deepest at linear O–NNO geometry, but its barrier to product is also high. When O–NNO is bent, the well becomes shallower, but the barrier to product is also reduced significantly. This entrance well is broad in terms of orientation angle of the attacking $O(^1D)$ atom and covers about a hemisphere at the N end of the N_2O reactant.[17]

A *trans*-bent ONNO intermediate has been located by CASSCF(18*e*,14*o*) method.[15] At the CASPT2 refined energy, this intermediate is 65.8 kcal/mol lower than the reactant and the barrier to product is about 3.6 kcal/mol. A *cis*-bent ONNO intermediate has also been found. Its energy is significantly higher than the *trans* isomer, suggesting that it should be less important for (R1).[15]

In both high level PES calculations, there is no significant entrance well for (R2) and the potential energy drop at the exit valley is very large.[15,17] The energy release at the exit valley should correlate to the product energy partitioning. The reaction coordinate of (R2) near the exit region is quite parallel to the bond length of the breaking NN–OO bond with only small variations of the bending angles.[14,17] It is thus expected that the majority of the energy release should be transferred to the product translational energy. On the other hand, the energy release at the entrance valley should be transferred to vibrational motions of the intermediate and thus contributes less to the product translational energy. Besides stretching motions, bending motions should be extensively involved in (R1) because of significant variations of bending angles along the minimum energy path.[15,17]

Both (R1) and (R2) have nonsymmetric product angular distributions, indicating that the lifetime of the reaction intermediate (if it exists) is shorter than its rotational period. (R1) has at least one stable intermediate.[15] However, its lifetime is expected to be short because the barrier height to products is small. For (R2), the barrier to products is either nonexistent or negligible,[15,17] suggesting even faster reaction time scales. Forward scattered products can easily be accounted for by contributions from large impact parameters as there is no potential energy barrier in the entrance region. Both minimum energy paths of (R1) and (R2) involve nonlinear geometries, which could smear out the product angular distributions.

From the $P(E)$'s in Figs. 4 and 6, we can calculate the average kinetic energy release $\langle E_T \rangle$ and the translational fraction of the available energy, $f_T=\langle E_T \rangle / E_{avl}$. Here the available energy E_{avl} is the sum of the collision energy and the reaction exothermicity. Table I summarizes the product energy partitioning of (R1) and (R2). The average product vibrational energy of (R2) is from a QCT calculation. All other values are from various experimental measurements. There is a large discrepancy in literature values for the product vibrational distribution of (R1). Pisano *et al.*[13] measured the NO vibrational distribution using a REMPI method in a single molecular beam. They reported a much higher vibrational excitation than other studies. Their average total product vibrational energy has a lower bound of 24 000 cm^{-1}, corresponding to $f_V \geqslant 0.75$.[13] From our experimental data, we determined $f_T=0.31$. If this $f_V \geqslant 0.75$ is right, f_R has to be almost zero to balance the energy partitioning, considering possible error bars of both f_V and f_T. However, small f_R is not likely. High rotational excitation of the NO product in $v=0-6$ has been observed by several groups.[4,5,9,12]

Brouard *et al.*[5] suggested two (limiting) types of reaction mechanisms: one a direct "stripping" reaction yielding NO $(v=0)+NO(v=16-18)$ and the other an indirect process in which the collision complex survives for a sufficient time to allow energy redistribution, leading to the formation of rotationally hot NO in $v=1-15$. However, the relative yield of the stripping mechanism is only supported by the observed large signal of NO $(v=0)$.[5] By energy balance, this particular product channel of NO $(v=0)+NO(v=16-18)$ must have small translational energy. The yield of this particular channel should be minor according to our experimentally derived $P(E_T)$ in Fig. 4 as it is peaked away from zero. The NO $(v=0)$ signal could be easily contaminated by background NO gas, consistent with the observation that the

TABLE I. Comparison of the product energy partitioning ($\langle E_T\rangle$, $\langle E_R\rangle$, and $\langle E_V\rangle$ are in kcal/mol).

Channel	$\langle E_T\rangle$	$\langle E_R\rangle$	$\langle E_V\rangle$	f_T	f_R	f_V	Reference (method, condition)
R1	28.0			0.31[a]			This work (TOF, crossed beam)
			32.1			0.37[b]	7 (LIF, cell)
			68.6–80.1[c]			0.75–0.87[c]	13 (REMPI, single beam)
		21.2(v=1–6)[d]	33.4[e]			0.35[f]	12 (TR-FT-IR, cell)
			33.8[e]			0.36[f]	11 (FT-IR, cell)
		39.7(v=0–2)[g]					9 (LIF, cell)
R2	62.5			0.57[a]			This work (TOF, crossed beam)
			(38.3)			(0.33)[f]	11 (QCT calculation)

[a]E_{av1}(R1)=89.7 kcal/mol, E_{av1}(R2)=110.1 kcal/mol, and E_c=7.8 kcal/mol.
[b]E_{av1}(R1)=87.0 kcal/mol.
[c]E_{av1}(R1)=91.5 kcal/mol.
[d]10.6 kcal/mol per NO molecule, partially relaxed.
[e]Population of NO(v=0) was assumed by extrapolating. Here we pick $P(v=0)=1.2P(v=1)$.
[f]E_{av1}(R1)=94.5 kcal/mol, $\langle E_c\rangle$=12.6 kcal/mol, E_{av1}(R2)=118.4 kcal/mol, E_c=16.1 kcal/mol.
[g]19.9 kcal/mol per NO molecule.

NO (v=0) in their measurement is translationally and rotationally much colder than other vibrational levels.[5] Furthermore, recent LIF studies show that NO (v=0,1,2) products are highly rotational excited.[9] Full determination of the NO rotational distribution is difficult due to very fast rotation-to-translation relaxation rates. A time-resolved FT-IR emission study[12] gives a lower bound of average rotational energy of ~3700 cm^{-1} (population-weighted average over v=1–6), in which partial rotational relaxation is likely under the experimental condition. The LIF study[9] shows much higher average rotational energies ranging from 6300 to 7500 cm^{-1} for v=0,1,2. Shorter delay time in the LIF detection should reduce the probability of rotational relaxation. NO (v=0–6) already covers the majority (>80%) of the vibrational population.[7,11,12] If we take the f_V=0.37 from Ref. 7 and our f_T=0.31, we can deduce f_R=0.32, that is, the average total rotational energy is about 29 kcal/mol (~10 000 cm^{-1}). The pair correlation of the two NO molecules is not clear yet. If they share the rotational energy about evenly, each NO molecule should have ≈5000 cm^{-1} average rotational energy, which is roughly consistent with Refs. 9 and 12, considering that only very low vibrational levels are probed in Ref. 9 and partial rotational relaxation is likely in Ref. 12. As the yield of the stripping mechanism should be minor, a short-lived complex should be responsible for the major mechanism of (R1). The lifetime of the collision complex should be less than its rotational period as suggested by the asymmetric $P(\theta)$ in Fig. 4. Energy redistribution in the intermediate is very likely but not complete as evidenced by the observed vibrational and rotational distributions of the NO products.[7,9,12] The new NO is only moderately vibrationally hotter than the old NO.[7] Also, a statistical phase space theory can describe the major part of the rotational distribution for the NO (v=0,1,2) product.[9] It may be asked why the energy redistribution in the intermediate is more efficient than expected from the short lifetime and low barrier to product. The absence of hydrogen atom in this tetraatomic system may be one of the reasons, as the vibrational density of states is much higher than hydrogen containing systems of the same number of atoms.[9,25]

A direct mechanism for (R2) is expected from the lack of a potential energy well between the reactant and product and our data support this mechanism. Furthermore, a QCT calculation[11] has shown that the vibrational distribution of the $O_2(^1\Delta)$ product is very hot with v peaked at 9 while the N_2 product is extremely cold vibrationally. In contrast, the vibrational distribution of the new and old NO products from the same QCT calculation are broad and monotonically deceasing with an effective vibrational temperature of ~9000 K.[11]

From the relative signal intensities of the products of (R1) and (R2), we can deduce their relative yields. We have to compare the signal intensities in the CM frame, so the laboratory-CM transformation Jacobian factor has to be included. The cross sections[37] and cracking ratios of electron impact ionization at 70 eV are also taken into account.[38] The transmission efficiency of the quadrupole mass filter is assumed to be the same for mass 30, 32, 34, 44, and 46. For the branching ratio between (R1) and (R2), we used the signals at masses 32 ($^{32}NO^+$) and 34 ($^{34}O_2^+$) which should have very similar transmission efficiencies. After appropriate accounting for all of these sensitivity factors, we get the relative branching ratio of (R1): (R2) =62:38=1.6.

The NASA/JPL panel recommends the rate constants of (R1) and (R2) to be 6.7×10^{-11} and 4.9×10^{-11} cm^3 $molecule^{-1}$ s^{-1} at 298 K for use in stratospheric modeling studies,[39] in which the branching ratio of (R1): (R2) is 1.4. The IUPAC subcommittee evaluated the gas kinetic data for use in the studies of atmospheric chemistry and recommends that the rate constants are 7.2×10^{-11} and 4.4×10^{-11} cm^3 $molecule^{-1}$ s^{-1} at 298 K,[40] in which the branching ratio of (R1): (R2) is 1.6. It is very close to our result, although our collision energy of 7.8 kcal/mol is significantly higher than those at 298 K.

Takayanagi *et al.* investigated the collision energy dependence on this branching ratio by QCT calculation[17] as well as quantum-classical calculation[20] on the CASPT2 global surface. But the QCT calculation ignored the contribution of nonzero impact parameters; therefore, the branching ratio is only semiquantitative. The calculated branching ratio of

(R1): (R2) has a maximum value of ~1.3 at medium collision energies ranging from 4 to 8 kcal/mol and decreases at higher collision energies. The quantum-classical calculation shows a similar trend but somewhat smaller branching ratios with the maximum value of ~1.1. The room temperature data should represent the reaction events of low collision energies around 1 kcal/mol. The above calculated branching ratios at low collision energy range are about 1, which is significantly smaller than the room temperature experimental values recommended by both JPL and IUPAC. In contrast, a TST calculation based on CASPT2 transition state structures shows a fast rising branching ratio when the temperature is lowered.[15]

B. Isotope exchange channel

We have searched for the possibility of the isotope exchange channel, (R3), by measuring TOF spectra of mass 46 at a few laboratory angles, but we could not find any significant signal. The only TOF peak observed at mass 46 is likely from the elastic and inelastic scatterings of N_2O. A normal N_2O sample should have 0.2% $^{46}N_2O$ (natural abundance) which is also scattered by the O atom beam without any reaction and becomes background. We can simulate this contribution by scaling the TOF signal of mass 44 by the natural abundance of $^{46}N_2O$. If (R3) exists, the TOF signal should have this background subtracted. Experimentally, the signal is too weak to do the subtraction. Since the signal is likely smaller than the background, we can use the intensity of the background (scaled from the mass 44 TOF spectra) as the upper limit of (R3). After accounting for the appropriate laboratory-CM transformation Jacobian factor and relative detection efficiencies, we determined the upper limit of the branching ratio of (R3)/[(R1)+(R2)+(R3)] to be 0.8%. It suggests that the isotope exchange between N_2O and $O(^1D)$ is relatively unimportant, consistent with very recent literature.[32]

In the isotope exchange reaction of $O(^1D)+CO_2$, crossed molecular beam results show a long-lived collision complex mechanism.[26,27] RRKM calculation estimated the reaction time scale to be subnanosecond.[28] Although the electronic quenching isotope exchange process to produce $O(^3P)+CO_2$ is quite exothermic, it is relatively slow because it is spin forbidden. The nonquenching exchange process has been shown to be even slower, primarily due to small available energy and large density of states of the CO_3 complex. If the (presumed) isotope exchange reaction of $O(^1D)+N_2O$ is mechanistically similar to those of $O(^1D)+CO_2$, the expected rate should be also small and could not compete with the very fast (R1) and (R2).

IV. CONCLUSION

We have studied the $O(^1D)+N_2O$ reaction at 7.8 kcal/mol collision energy using the crossed molecular beam technique. Three product channels, NO+NO (R1), N_2+O_2 (R2), and isotope exchange reaction (R3), were investigated. By analyzing the product angular distributions and the product energy release in various degrees of freedom, the reaction mechanisms were discussed in detail. Discrepancy of the NO product vibrational distribution in the literature was discussed. A short-lived complex should be the major mechanism for the NO+NO channel. Although the lifetime is expected to be quite short, the couplings between vibrational modes in the entrance well/intermediate region may be strong enough to randomize large fraction of the available energy, resulting in statistical-like product energy distributions. On the other hand, the energy partitioning of the N_2+O_2 channel is highly nonstatistical. A very high fraction of translational energy release was observed, consistent with the shape of the potential energy surface. Finally, we have estimated the relative branching ratio of (R1):(R2) to be 62:38. The isotope exchange reaction (R3) was not observed in our sensitivity range (<0.8% in yield), suggesting that it is not important in the atmospheric isotope modeling.

ACKNOWLEDGMENTS

This work is supported by National Science Council, Taiwan (NSC94-2113-M-001-004) and Academia Sinica, Taipei, Taiwan. The authors like to thank Professor Yuan T. Lee for helpful discussions and A. L. Van Wyngarden for valuable comments on the manuscript.

[1] J. R. Wiesenfeld, Acc. Chem. Res. **15**, 110 (1982).
[2] N. Goldstein, G. D. Greenblatt, and J. R. Wiesenfeld, Chem. Phys. Lett. **96**, 410 (1983).
[3] G. A. Chamberlain and J. P. Simons, J. Chem. Soc., Faraday Trans. 2 **71**, 402 (1975).
[4] M. Brouard, S. P. Duxon, P. A. Enriquez, R. Sayos, and J. P. Simons, J. Phys. Chem. **95**, 8169 (1991).
[5] M. Brouard, S. P. Duxon, P. A. Enriquez, and J. P. Simons, J. Chem. Phys. **97**, 7414 (1992).
[6] K. Honma, Y. Fujimura, O. Kajimoto, and G. Inoue, J. Chem. Phys. **88**, 4739 (1988).
[7] H. Akagi, Y. Fujimura, and O. Kajimoto, J. Phys. Chem. **111**, 115 (1999).
[8] H. Akagi, Y. Fujimura, and O. Kajimoto, J. Chem. Soc., Faraday Trans. **94**, 1575 (1998).
[9] S. Kawai, Y. Fujimura, O. Kajimoto, and T. Takayanagi, J. Chem. Phys. **120**, 6430 (2004).
[10] H. Tsurumaki, Y. Fujimura, and O. Kajimoto, J. Chem. Phys. **111**, 592 (1999).
[11] X. B. Wang, H. Z. Li, Q. H. Zhu, F. N. Kong, and H. G. Yu, J. Chin. Chem. Soc. (Taipei) **42**, 399 (1995).
[12] G. Hancock and V. Haverd, Phys. Chem. Chem. Phys. **5**, 2369 (2003).
[13] P. J. Pisano, M. S. Westley, and P. L. Houston, Chem. Phys. Lett. **318**, 385 (2000).
[14] I. Last, A. Aguilar, R. Sayós, M. González, and M. Gilibert, J. Phys. Chem. A **101**, 1206 (1997).
[15] M. González, R. Valero, J. M. Anglada, and R. Sayós, J. Chem. Phys. **115**, 7015 (2001).
[16] H. Akagi, A. Yokoyama, Y. Fujimura, and T. Takayanagi, Chem. Phys. Lett. **324**, 423 (2000).
[17] T. Takayanagi and H. Akagi, Chem. Phys. Lett. **363**, 298 (2002).
[18] R. Sayós, R. Valero, J. M. Anglada, and M. González, J. Chem. Phys. **112**, 6608 (2000).
[19] M. A. Vincent, I. H. Hillier, and L. Salsi, Phys. Chem. Chem. Phys. **2**, 707 (2000).
[20] T. Takayanagi, Chem. Phys. **308**, 211 (2005).
[21] T. Takayanagi and A. Wada, Chem. Phys. **269**, 37 (2001).
[22] M. Ben-Nun, M. Brouard, J. P. Simons, and R. D. Levine, Chem. Phys. Lett. **210**, 423 (1993).
[23] M. González, R. Sayós, P. A. Enríquez, D. Troya, and M. P. Puyuelo, Faraday Discuss. **108**, 427 (1997).
[24] M. González, D. Troya, M. P. Puyuelo, R. Sayós, and P. A. Enríquez, Chem. Phys. Lett. **300**, 603 (1999).
[25] H. Akagi, Y. Fujimura, and O. Kajimoto, J. Chem. Phys. **110**, 7264 (1999).
[26] M. J. Perri, A. L. Van Wyngarden, K. A. Boering, J. J. Lin, and Y. T. Lee,

J. Chem. Phys. **119**, 8213 (2003).
[27] M. J. Perri, A. L. Van Wyngarden, K. A. Boering, J. J. Lin, and Y. T. Lee, J. Phys. Chem. A **108**, 7995 (2004).
[28] A. M. Mebel, M. Hayashi, V. V. Kislov, and S. H. Lin, J. Phys. Chem. A **108**, 7983 (2004).
[29] Y. L. Yung, M. C. Liang, G. A. Blake, R. P. Muller, and C. E. Miller, Geophys. Res. Lett. **31**, L19106 (2004).
[30] T. Rockmann and J. Kaiser, Geophys. Res. Lett. **32**, L11807 (2005).
[31] Y. L. Yung, M. C. Liang, G. A. Blake, R. P. Muller, and C. E. Miller, Geophys. Res. Lett. **32**, L11808 (2005).
[32] J. Kaiser and T. Rockmann, Geophys. Res. Lett. **32**, L15808 (2005).
[33] J. A. Davidson, C. J. Howard, H. I. Schiff, and F. C. Fehsenfeld, J. Chem. Phys. **70**, 1697 (1979).
[34] S. Nishida, K. Takahashi, Y. Matsumi, N. Taniguchi, and S. Hayashida, J. Phys. Chem. A **108**, 2451 (2004).
[35] NIST kinetic database, http://kinetics.nist.gov/index.php
[36] U. Even, J. Jortner, D. Noy, N. Lavie, and C. Cossart-Magos, J. Chem. Phys. **112**, 8068 (2000).
[37] http://physics.nist.gov/PhysRefData/Ionization/
[38] Mass spectra of NO and O_2 are from the NIST chemistry webbook (http://webbook.nist.gov); the available cracking ratios are for room temperature samples. Because NO^+ and O_2^+ both have strong bond energy, the extent of cracking is small and its dependence on the product internal excitation is expected to be small, which should not be a significant factor for the branching ratio determination.
[39] S. P. Sander, R. R. Friedl, D. M. Golden *et al.*, Evaluation No. 14, JPL Publication No. 02-25, 2003 (JPL, Pasadena, CA, 2003).
[40] R. Atkinson, D. L. Baulch, R. A. Cox, R. F. Hampson, Jr., J. A. Kerr, M. J. Rossi, and J. Troe, J. Phys. Chem. Ref. Data **26**, 521 (1997).